

RESULTS AND FUTURE USES OF HETERODYNE SPATIAL INTERFEROMETRY AT 11 MICRONS*

Edmund C. Sutton

Department of Physics, University of California, Berkeley

ABSTRACT

Heterodyne spatial interferometry at a wavelength of 11 microns has been used to examine properties of circumstellar dust shells. Among the objects which have been observed are several M-type supergiants and Mira variables as well as several peculiar infrared stars. These measurements provide information on the temperature and spatial distribution of dust grains. Possible future developments in heterodyne interferometry include longer baselines for higher resolution and the use of larger telescopes for greater sensitivity.

1. INTRODUCTION

Recent advances in infrared interferometry have been largely motivated by the desire to study the physical properties of circumstellar dust shells. Such dust shells are common features of cool, late-type stars, and thermal emission from this dust is often a strong source of infrared radiation. At wavelengths near 10 microns thermal emission by silicate grains is particularly strong due to the presence of an emission feature in the spectra of these grains. Properties such as the temperature and spatial distribution of the dust have remained largely unknown, and it is the purpose of interferometry to understand these properties by studying the spatial distribution of the infrared radiation.

Interferometric approaches to this problem have consisted of the heterodyne work discussed here and the direct interference of infrared beams as used by McCarthy, Low and Howell¹. Heterodyne work has had the advantage of higher resolution whereas the direct interference has had greater sensitivity. There are other types of measurements where heterodyne interferometry has a

*This work is supported in part by NASA Grant NGL 05-003-272 and NSF Grant AST 77-12256

particular advantage. The heterodyne system allows in principle for measurement of the complex fringe visibility of a source, that is the phase as well as the amplitude of the interference signal. Consequently, aperture synthesis maps may be constructed with a heterodyne interferometer, and such mapping may be done with a multiple telescope array. The measurement of phase also allows for accurate astrometric positional measurements. One final unique advantage of heterodyne techniques is that they are easily adaptable for very long baselines. For example, baselines of the order of 100 meters in length with resolutions of the order of 0.01 seconds of arc seem feasible. It is in applications of these sorts that the advantages of heterodyne interferometry become quite considerable.

2. INTERFEROMETER DESIGN

The interferometer presently in use at Kitt Peak National Observatory consists of two telescopes, two separate heterodyne receivers, and circuitry which correlates the outputs of the receivers and records the interference signal. The telescopes used are the twin 81 cm diameter McMath auxiliary telescopes which are separated by a 5.5 meter east-west baseline. At an operating wavelength of 11.1 microns, this gives a fringe spacing at transit of 0.4 seconds of arc.

The heterodyne receivers are shown in simplified form in Figure 1. The principle of heterodyne reception involves the physical superposition of the radiation fields from two different sources. Here the radiation from a CO₂ laser local oscillator is combined with the infrared stellar radiation collected by the telescope. This is then focused onto a HgCdTe photodiode, which is at liquid nitrogen temperature. The electric field at the surface of the photomixer is thus described by

$$\vec{E}_{TOT} = \vec{E}_L e^{i\omega_L t} + \vec{E}_S e^{i(\omega_S t + \phi(t))}. \quad (1)$$

The first term, representing the laser field, is much stronger than the signal field. The laser radiation contains only the fixed frequency ω_L whereas the signal contains power over a wide range of frequencies ω_S . The photocurrent

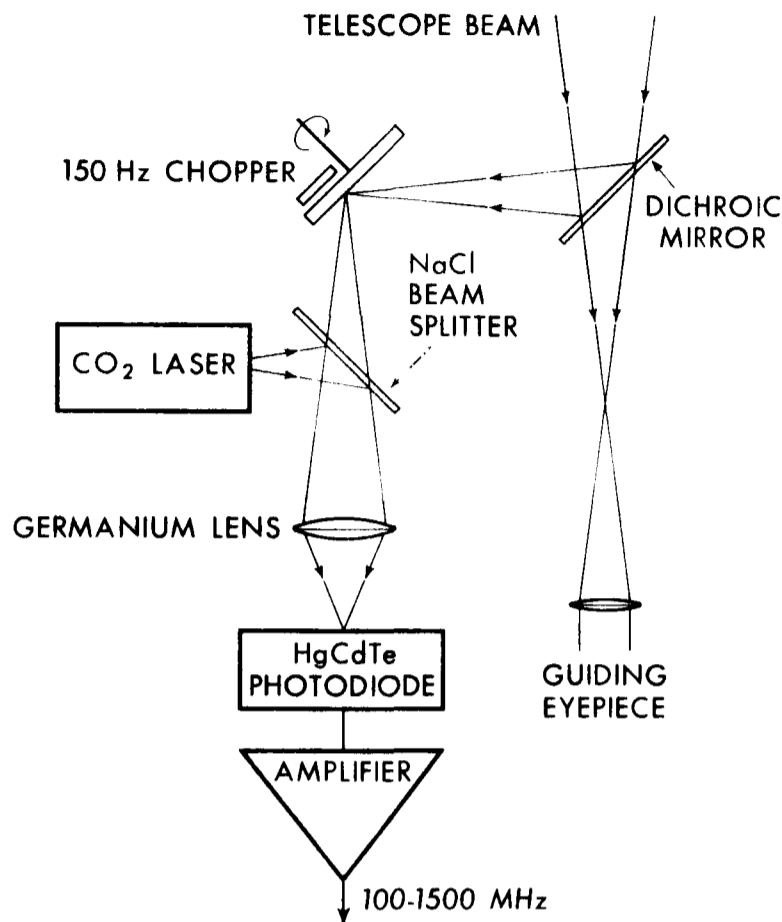


Figure 1: Schematic diagram of a heterodyne receiver.

in the detector is then proportional to the modulus-squared of the total electric field:

$$i_{\text{PHOT}} \propto |E_L|^2 + |E_S|^2 + 2\vec{E}_L \cdot \vec{E}_S \cos\{(\omega_L - \omega_S)t - \phi(t)\}. \quad (2)$$

The heterodyne signal is the last term in this equation. It contains signals at intermediate frequencies from near DC out to the detector bandwidth $\Delta\nu_{\text{IF}}$. For the detectors presently in use, this intermediate frequency bandwidth is 1400 MHz. The infrared bandwidth is twice this due to the detection of infrared radiation in bands of this width both above and below the laser frequency.

The signal-to-noise ratio of a heterodyne receiver is essentially

$$\frac{S}{N} = \frac{\eta P_s}{h\nu \Delta\nu_{\text{IF}}} \sqrt{\Delta\nu_{\text{IF}} \cdot t_{\text{INT}}}. \quad (3)$$

Here P_s is the source power in the bandwidth $\Delta\nu_{\text{IF}}$, η is the effective quantum efficiency, and t_{INT} is the integration time. The effective quantum efficiency of the receivers are at present about 25%, which implies a sensitivity of 3×10^{-15} watts in a 1 second integration.

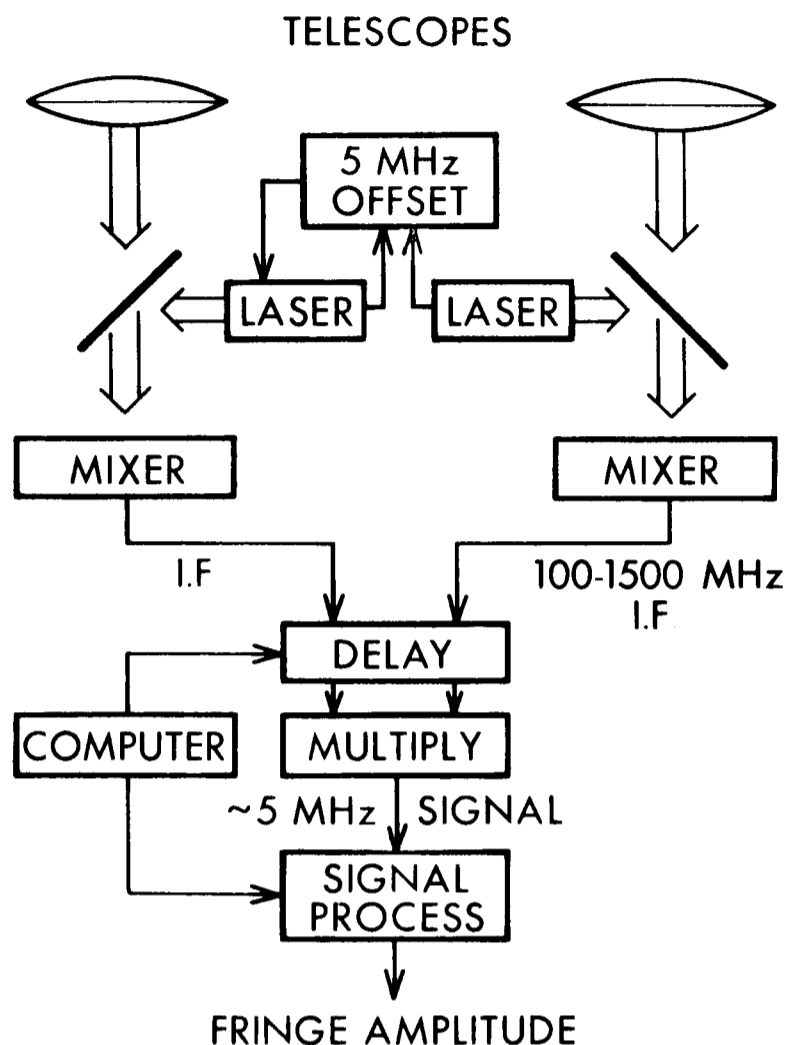


Figure 2: Interferometer constructed from two heterodyne receivers.

The interference signal is obtained by multiplying the outputs of the heterodyne receivers as is shown in Figure 2. The signals are first sent through a variable-length delay-line to equalize the total signal path length in the two receivers. This equalization must be done to an accuracy much better than the reciprocal of the receiver bandwidth. For the relatively narrow bandwidths employed here this is 10 cm, and it is easy to achieve an accuracy much better than this. Finally, the interference signal is digitized and recorded on magnetic tape for later analysis.

Information about the brightness distribution of a source is obtained by observations at a variety of hour angles. For these different measurements the projected length of the baseline varies, and thus a variety of resolutions are obtained. The fringe visibility as a function of spatial frequency is the Fourier transform of the source brightness distribution. Consequently, models of the brightness distribution can be transformed and compared with the observations. A commonly used model is that of a uniform circular disk. However, this model produces a series of subsidiary maxima in the visibility curves

which in general seem to be absent, indicating that this is a rather oversimplified and unphysical model for most infrared sources. Instead dust shells are likely to be more tapered and should gradually become fainter at larger radii as the dust becomes thinner and cooler. For this reason, Gaussian brightness distributions seem to be somewhat more reasonable and are adequate models where the data is not sufficient to more precisely define the shape of the distribution.

Observations with the heterodyne interferometer have consisted of discrete integrations varying in length from 500 to 2000 seconds. The power in the interference signal integrated over a bandwidth wider than the frequency spread due to atmospheric seeing effects is compared with the signals obtained using the two telescopes as individual total-power receivers. The resulting normalized amplitude of the interference signal is simply the modulus of the fringe visibility.

As a check of the instrumental calibration, observations were made of the star α Her, which is the brightest 11 micron source without any significant amount of silicate emission. Thus it is expected to behave as a point source, and indeed a set of four observations of α Her yielded a visibility of 0.97 ± 0.07 , confirming the calibration.

3. SUMMARY OF RESULTS

Over the course of the past two years, observations have been made for ten different sources including various M-type supergiants, Mira variables, and other peculiar infrared stars. These objects exhibit a variety of features which help to determine properties of circumstellar dust. The results obtained on four of these objects for which the data is reasonably extensive are presented here.

α Ori is the most easily studied of the simple M-type supergiants. It has an extensive gas and dust cloud^{2,3}, and a significant fraction of its 11 micron radiation comes from thermal emission by circumstellar silicate grains. The data presented in Figure 3 represent the best and most recent heterodyne measurements of the visibility of α Ori, and they are in good

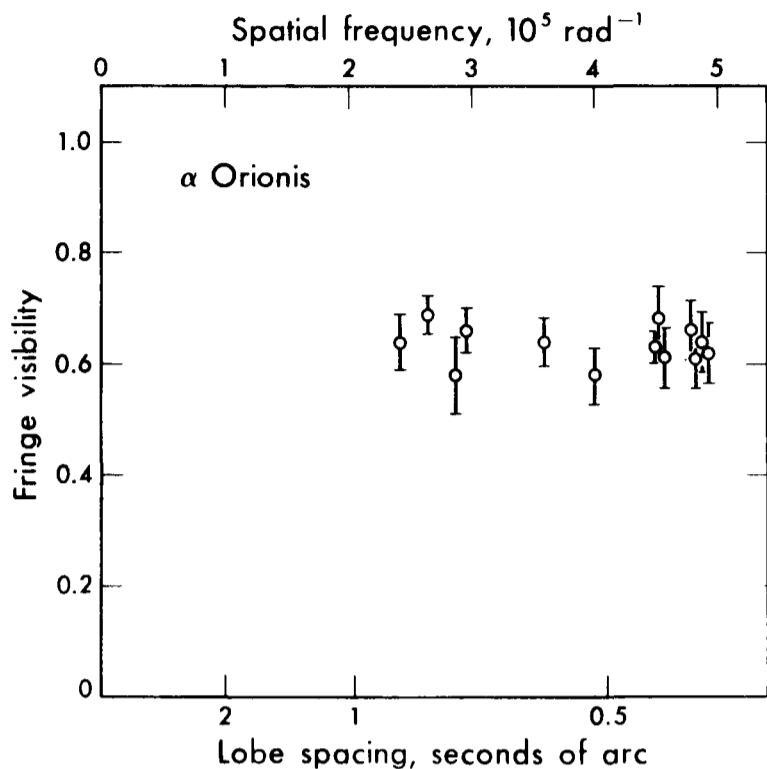


Figure 3: Fringe visibility measurements of α Ori. Only the best and most recently acquired data are presented.

agreement with the values previously reported by Sutton, et al⁴ as well as the independent work of McCarthy, Low and Howell¹.

The most striking feature of this data is the extreme flatness of the visibility curve over a factor of two range in spatial frequency. This indicates that the brightness distribution is divided into two distinct components: one of which is unresolved at these resolutions and one of which is overresolved. These components are the photospheric contribution and the dust contribution respectively, and the value of the visibility across the flat region is consistent with the ratio of the brightnesses of these components known from photometric measurements^{5,6}. The fact that the dust shell is fully resolved indicates that it is at least $0.9''$ in diameter, and thus dust emission on the average must come from regions at least 18 stellar radii from α Ori. At this distance the temperature of a grain with a gray body emissivity spectrum would be about 550 K. Some fraction of the dust may be closer to the star than this, but the predominant region of dust emission is at this fairly large distance from α Ori.

Extensive observations have also been made of the Mira variable \omicron Ceti⁷. Figure 4 shows this data broken down into four sets of observations at various phases of the light cycle. This data is similar to that for α Ori in that it has a region of constant visibility, although here the increase in the

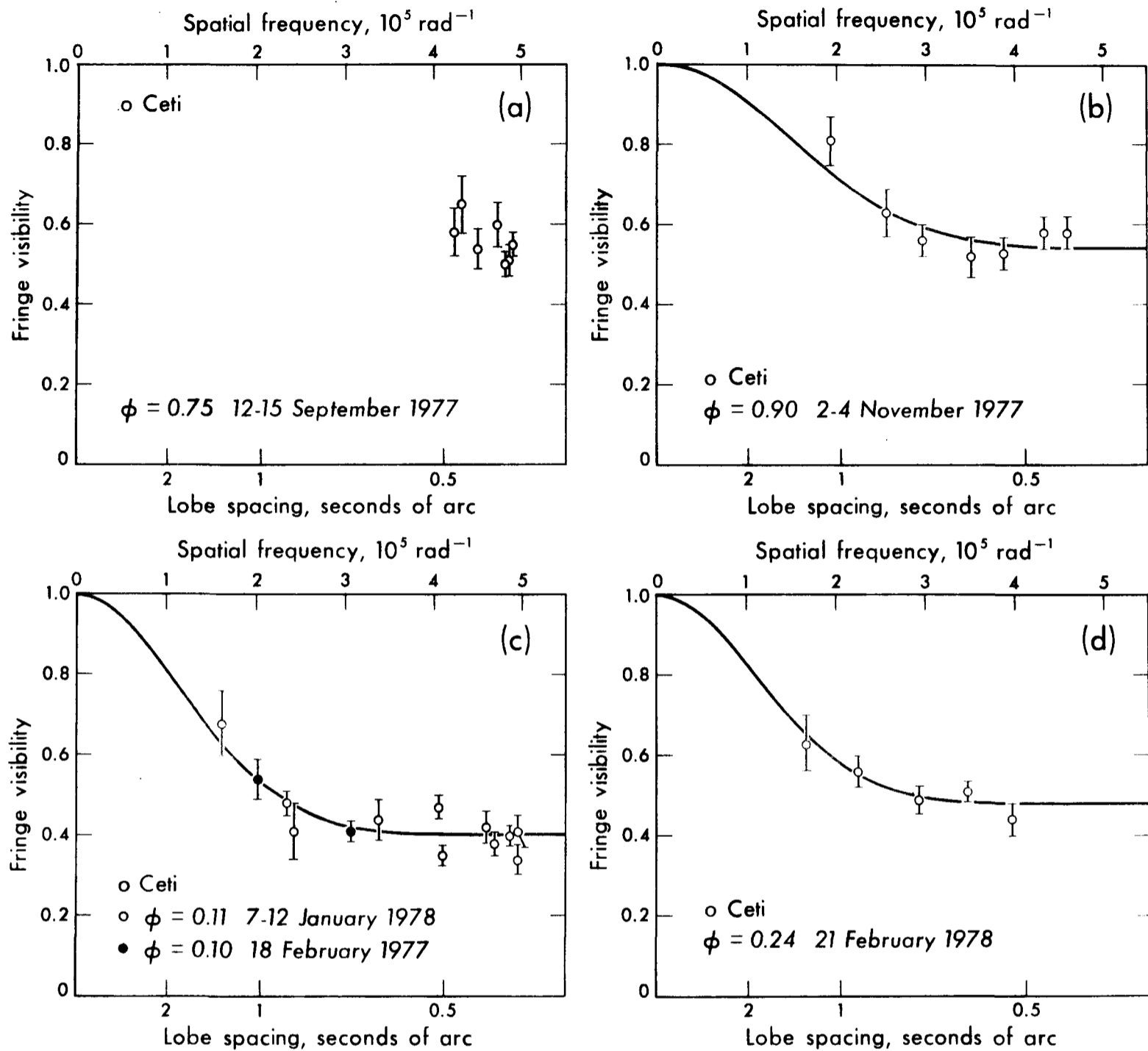


Figure 4: Fringe visibility measurements of \circ Ceti at four different phases of its visible light cycle (From Sutton, et al⁷)

visibility at low resolutions due to the presence of the dust is evident. The diameter of the dust shell in these cases is approximately $0.7''$. At this distance dust temperatures of 400 K are expected. Reasonable radial variations of temperature and density will allow for the presence of some dust sufficiently close to the star to be at about 700 K, although dust closer than this is unlikely.

Another interesting feature is apparent in comparing the observations at various phases, and that is that the value of the visibility in the flat part of the curve at high spatial frequency varies with phase. This means that changes have occurred in the relative brightnesses of the dust shell and the photospheric emission. The visibility is least, and thus dust emission is strongest, in curve "C" which occurs closest to the period of maximum stellar luminosity. This change in contrast between dust emission and photospheric emission may be understood in terms of changes in dust grain temperature. As the star becomes hotter the stellar 11 micron brightness increases. Simultaneously, the dust grains are heated and their brightness increases even more rapidly in accordance with the Planck distribution. The size of the change in contrast between these two components is a measure of the average dust grain temperature. The effect shown here is explained by grains at a characteristic temperature of 300 K and allows for some grains as warm as 500-700 K balanced by some cooler grains. This result is consistent with the value for the temperature determined from the size of the dust shell. McCarthy, Howell and Low⁸ have also made measurements of the brightness distribution of α Ceti. There exist differences between their data and that presented here, but the interpretations are somewhat similar.

The heavily obscured variable star VY Canis Majoris is an interesting object for interferometry since virtually all of its 11 micron radiation comes from dust emission. The data on this object as previously presented by Sutton, et al⁴ are shown in Figure 5. At highest resolution, this source is almost completely resolved except for about 8% of the total flux. The remainder may be modelled by a Gaussian spatial distribution whose full width to 1/e intensity is $0.58'' \pm 0.04''$.

The extremely bright source IRC +10216 is similar to VY Canis Majoris in that it has an optically thick dust shell which dominates its spectrum at infrared wavelengths. It is different from VY Canis Majoris in one very important manner, which is that the central object in IRC +10216 is thought to be a carbon star. This being the case, the nature of the dust particles is likely to be quite different. Graphite rather than silicate particles are expected to be the dominant species of dust near carbon stars. Recent

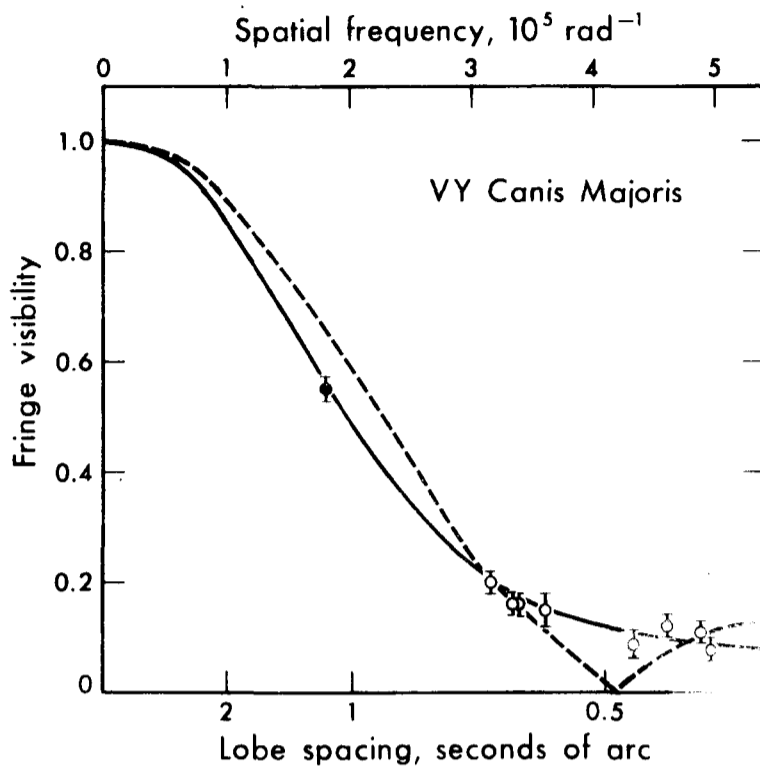


Figure 5: Fringe visibility measurements of VY Canis Majoris. The filled circle is from McCarthy, Low and Howell¹. The solid line is the best fit to the data as discussed in the text (From Sutton, et al⁴).

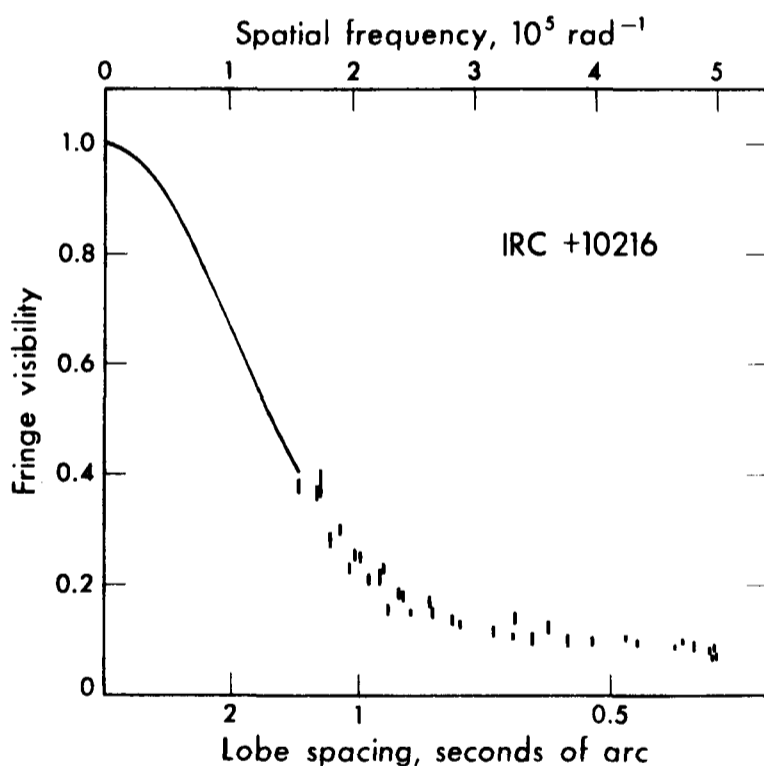


Figure 6: Preliminary measurements of the fringe visibility of IRC +10216. The lengths of the bars are 2σ .

observations of this source are shown in Figure 6. Several interesting features are evident. The unresolved component contains about 10% of the flux and must be smaller than $0.2''$. If this represents emission from the central star, the optical depth of the shell can not be too much greater than 1. The bulk of the dust emission comes from a component $0.8''$ in diameter. This is distinctly different than the two shell model of Toombs, et al⁹, which was derived from a lunar occultation measurement.

These various measurements of circumstellar dust shells have provided new information about the properties of such dust. This should help to improve our understanding both of the formation of dust grains and of the characteristics of late-type stars.

4. THE FUTURE OF INFRARED HETERODYNE INTERFEROMETRY

Heterodyne interferometry at infrared wavelengths has advanced to the point where it is possible to make fairly definite predictions about its future applications. Among those applications will clearly be more detailed studies of the properties of circumstellar dust of the sort that have been described here. In order to see what other uses heterodyne interferometry may have, it is helpful to consider the changes and improvements in the interferometer which may be made in the future.

IMPROVEMENTS IN HETERODYNE INTERFEROMETRY

	<u>GAIN IN SENSITIVITY</u>
<u>RECEIVER SENSITIVITY:</u>	
OPTICAL TRANSMISSION	1.15
AMPLIFIER NOISE	1.25
DETECTOR QUANTUM EFFICIENCY	1.5
<u>WAVEFRONT MATCHING EFFICIENCY</u>	
(PPOINT SOURCE)	1.1
60-INCH DIAMETER TELESCOPES	4
LONGER BASELINE AND DIFFERENT ORIENTATIONS	—
COHERENCE TIME (1000 sec vs 1 sec)	6

Table 1

A list of such possible improvements is provided in Table 1. The first group of these are associated with the sensitivities of the heterodyne receivers. The receivers in use at this time are approximately a factor of 4 less sensitive than the quantum noise limit for the bandwidth and wavelength used. Some improvement is possible with relatively little difficulty. For example, replacing some of the optics in the receivers would bring about a 15% increase in optical transmission and hence sensitivity. Other types of improvement will depend on anticipated technological developments in several fields. At present there is a contribution of excess noise from the radio-frequency amplifiers used to amplify the signals out of the detectors. Perfect amplifiers would increase the signal-to-noise ratio of the receivers by 25%. Significant

advances in the technology of making such amplifiers are occurring at the present time, and it seems likely that a large fraction of this possible improvement will occur within a couple of years. Also some of this gain can be realized without improving the amplifiers simply by improving the efficiency of coupling the detector's radio-frequency output into the amplifiers.

The technology of HgCdTe photodiodes is also a rapidly developing field. The detectors presently used in the interferometer have an effective heterodyne quantum efficiency of approximately 0.40 over a bandwidth of 1400 MHz. Detectors are already being made which approach 50% quantum efficiency, and 60% should be possible within the next few years¹⁰. A wider detector bandwidth would also improve sensitivity, but the expected gains are smaller and less certain and have not been included in the table. In addition to the improvements to receiver sensitivity, it seems that there is at least 10% to be gained in the efficiency of coupling the receiver to the telescope. These four factors combined give a factor of 2.4 increase in sensitivity; this is the degree of improvement which should be possible with the present system within a few years.

Other much greater improvements are possible with more major changes in the interferometer. For example, an increase in telescope size would be beneficial since the sensitivity of a heterodyne receiver is directly proportional to the collecting area of the telescope used as long as the wavefront from a stellar source is coherent over the aperture. Studies of atmospheric coherence in the infrared by Boyd¹¹ have shown that under moderately good seeing conditions (2" in the visible) 60" apertures should be coherent at 11 microns, and Betz¹² has observed the expected fourfold increase of signal with a heterodyne receiver in going from a 30" to a 60" telescope.

Another major gain would be to have an interferometer whose baseline is flexible both in length and orientation. Here the goal is not sensitivity but the additional information about a source's brightness distribution which can be obtained. Such flexibility is a natural property of a heterodyne interferometer since the spacing and positioning of the telescopes in principle may be arbitrarily varied. So far, spatial resolution has been limited by the 5.5 meter length of the present baseline. Additional resolution would be

helpful, particularly in order to measure the sizes of the compact components in IRC +10216 and VY Canis Majoris. A variable baseline orientation allows information to be obtained about the departure from circular symmetry which is likely to be present in rotating dust clouds. To some extent the orientation of a fixed baseline is varied by the earth's rotation, but the usefulness of this effect is limited since the angle through which the baseline is rotated is often quite small, it cannot be chosen at will, and such rotation occurs only in conjunction with simultaneous changes in baseline length.

Yet another area for major improvement is in the phase stability of the interference signal. Phase fluctuations are caused by atmospheric "seeing" effects as well as local turbulence within the telescope structure. The McMath auxiliary telescopes are particularly bad with respect to local turbulence since they each have a confined optical path of approximately 120 meters, which contributes a significant fraction of the observed fluctuations. This local contribution to the phase fluctuations need not be present in a well designed interferometer system. The atmospheric contribution is less easily controlled beyond choosing a site for interferometry with good seeing. At present the phase of the interference signal generally stays stable only for about 1 second although coherence times of 1000 seconds have been observed under good seeing conditions¹³ If such coherence times can be achieved routinely, the sensitivity in measuring the amplitude of an interference signal will be increased by a factor of 6 (the fourth root of the ratio of coherence times). In addition, long-term coherence raises the interesting possibility of making accurate positional measurements by means of the phase of the interference signal.

The improvements listed here allow for a number of new applications for infrared heterodyne interferometry and for extension of the present measurements with greater sensitivity. The most exciting and different of those possible applications are associated with phase-sensitive positional measurements and with the use of much longer and variable baselines. Thus the future of heterodyne interferometry through the next few years seems quite promising.

REFERENCES

- 1) D.W. McCarthy, F.J. Low, and R. Howell, *Astrophys. J. Lett.*, 214, L85, 1977.
- 2) A.P. Bernat and D.L. Lambert, *Astrophys. J. Lett.*, 201, L153, 1975.
- 3) H.M. Dyck and T. Simon, *Astrophys. J.*, 195, 689, 1975.
- 4) E.C. Sutton, J.W.V. Storey, A.L. Betz, C.H. Townes, and D.L. Spears, *Astrophys. J. Lett.* 217, L97, 1977.
- 5) F.C. Gillett, K.M. Merrill, and W.A. Stein, *Astrophys. J.*, 164, 83, 1971.
- 6) K.M. Merrill and W.A. Stein, *Publ. Astron. Soc. Pac.*, 88, 285, 1976.
- 7) E.C. Sutton, J.W.V. Storey, C.H. Townes, and D.L. Spears, *Astrophys. J. Lett.*, in press, 1978.
- 8) D.W. McCarthy, R. Howell, and F. J. Low, *Astrophys. J. Lett.* 223, L113, 1978.
- 9) R.I. Toombs, E.E. Becklin, J.A. Frogel, K.S. Law, F.C. Porter, and J.A. Westphal, *Astrophys. J. Lett.*, 173, L71, 1972.
- 10) D.L. Spears, private communication.
- 11) R.W. Boyd, *J. Opt. Soc. Amer.*, in press, 1978.
- 12) A.L. Betz, private communication.
- 13) C.H. Townes, E.C. Sutton, and J.W.V. Storey, Optical Telescopes of the Future. Conference Proceeding, Dec. 1977. Geneva 23: ESO c/o CERN 1978.

DISCUSSION

D.L. Fried: You have given the sensitivity improvement factor for an increase in coherence time as the fourth root of the increase. Why isn't it a square root dependence?

E.C. Sutton: Our integration time is generally much larger than the atmospheric coherence time. For a fixed integration time the sensitivity increases as the fourth root of the coherence time as long as this coherence time remains shorter than the length of the integration.

D.W. McCarthy Jr.: Discuss the sources of error and observed repeatability in your observations. In particular, what do the error bars in visibility measurements of α Ceti represent and how do you explain the different results obtained for α Ceti at lobe spacing $0.5''$ in Figure 4(c)?

E.C. Sutton: The error bars are $\pm\sigma$ and represent the statistical uncertainties due to receiver noise. The repeatability is best shown in the data for α Ori where observations spaced over a period of about one year are included. In fact, all of the figures show data from more than one night which are interleaved. For \circ Ceti the two points referred to are from separate nights; during both nights several of the other data points were obtained. There is no overall systematic difference between the two nights and nothing else which otherwise distinguishes these points.

P.B. Boyce: Does your analysis assume circular symmetry of the source?

E.C. Sutton: We don't assume circular symmetry, rather we have obtained information about the brightness distribution along a particular axis which is given by the orientation of the projected baseline. In general, some change in this orientation is provided by the Earth's rotation. This effect is combined with changes in baseline length, but it is possible to compare observations on both sides of transit for which the projected baseline lengths are the same but the orientations different. This will allow us to measure the degree of circular symmetry of various sources.